

Using Spectral Estimation Techniques in Adaptive Processing Antenna Systems

WILLIAM F. GABRIEL, FELLOW, IEEE

Abstract—Improved spectral estimation techniques hold promise for becoming a valuable asset in adaptive processing array antenna systems. Their value lies in the considerable amount of additional useful information which they can provide about the interference environment, utilizing a relatively small number of degrees of freedom (DOF). The “superresolution” capabilities, estimation of coherence, and relative power level determination serve to complement and refine the data from faster conventional estimation techniques. Two conceptual application area examples for using such techniques are discussed; partially adaptive low-sidelobe arrays, and fully adaptive tracking arrays. For the partially adaptive area the information is utilized for efficient assignment of a limited number of DOF in a beamspace constrained adaptive system in order to obtain a stable main beam, retention of low sidelobes, considerably faster response, and reduction in overall cost. These benefits are demonstrated via simulation examples computed for a 16-element linear array. For the fully adaptive tracking array area the information is utilized in an all-digital processing system concept to permit stable nulling of coherent interference sources in the main beam region, efficient assignment/control of the available DOF, and greater flexibility in time-domain adaptive filtering strategy.

I. INTRODUCTION

IMPROVED SPECTRAL estimation techniques are an emerging technology which derives largely from modern spectral estimation theory of the past decade and adaptive array processing techniques [2], [3], [4]. Coupled with the phenomenal advances in digital processing [5], these techniques are becoming a valuable asset for adaptive array antenna systems. Their value lies in the considerable amount of additional useful information which they can provide about the environment, utilizing only a relatively small number of degrees of freedom (DOF). For example, current spectral estimation algorithms can provide asymptotically unbiased estimates of the number of interference sources, source directions, source strengths, and any cross correlations (coherence) between sources [6], [7]. Such information can then be used to track and “catalogue” interference sources, hence assign adaptive DOF.

These newer techniques are not viewed as a “superresolution” replacement for more conventional estimation methods such as main beam search, analog beamformers, or spatial discrete Fourier transforms (DFT). Rather, the new technology is considered complementary to the other methods and best used in tandem. For example, “superresolution” tech-

niques cannot compete with the speed of a DFT. Some comparisons of the various methods may be found described in the literature [4], [7], [8].

The purpose of this paper is to present two conceptual application areas for using spectral estimation techniques; partially adaptive low-sidelobe antennas, and fully adaptive tracking arrays. A partially adaptive array is one in which only a part of the DOF (array elements or beams) are individually controlled adaptively [9], [10], [11]. Obviously, the fully adaptive configuration is preferred since it offers the most control over the response of the antenna system. But when the number of elements or beams becomes moderately large (hundreds), the fully adaptive processor implementation can become prohibitive in cost, size, and weight.

The paper is divided into three principal parts. Section II discusses partially adaptive, low-sidelobe antennas with the focus upon a constrained beamspace system; Section III considers source estimation and beam assignment from “superresolution” techniques; and Section IV discusses an all-digital, fully adaptive tracking array concept.

II. PARTIALLY ADAPTIVE LOW-SIDELOBE ANTENNAS

The antenna system addressed in this section is assumed to be a moderately large aperture array of low-sidelobe design wherein the investment is already considerable and one simply could not afford to make it fully adaptive. The assumption of low sidelobes (30 dB or better) is intended to give us good initial protection against modest interference sources and to reduce the problems from strong sources, i.e., in regard to the number of adaptive DOF required and the adaptive dynamic range of the processor. Thus, retention of the low sidelobes is considered a major goal in our adaptive system. In the discussion to follow, it is shown that using improved spectral estimation techniques in such a system can result in the following benefits over a fully adaptive array system.

- 1) Considerably faster adaptive response, reduction in computation burden, and reduction in overall cost because relatively few adaptive DOF are implemented.
- 2) Minimal degradation of both the main beam and sidelobe levels because simple adaptive weight constraints are made possible.
- 3) Compatible with a larger number of adaptive algorithms, including even analog versions.
- 4) Greater flexibility in achieving a “tailored” response due to greater information available.

On the negative side, a partially adaptive system can never be guaranteed a cancellation performance equal to that of a

Manuscript received May 3, 1985; revised September 16, 1985. This work was supported by NAVAIRSYSCOM and the Office of Naval Research. This paper is a condensation of NRL Rep. 8920 [1].

The author is with the Radar Division, Naval Research Laboratory, Washington, DC 20375.

IEEE Log Number 8407018.

fully adaptive array and, in addition, will deteriorate abruptly in performance when the interference situation exceeds its adaptive DOF. These risks are an inherent part of the package and must be carefully weighed for any specific system application.

A. A Low-Sidelobe Eigenvector Constraint

We begin this section by reviewing that unconstrained adaptive arrays can experience very "noisy" sidelobe fluctuations and main beam perturbations when the data observation/integration time is not long enough, even though the quiescent mainbeam weights are chosen for low sidelobes. Consider a linear array of K elements, with each element adaptively weighted, and let us compute the complex adaptive element weights W_k from the well-known sample matrix inverse (SMI) algorithm [11], [12]. Expressed in convenient matrix notation,

$$\mathbf{W} = \mu \hat{\mathbf{R}}^{-1} \mathbf{S}^* \quad (1)$$

where \mathbf{W} is the adaptive weights vector, $\hat{\mathbf{R}}$ is the sample covariance matrix, \mathbf{S}^* is the quiescent main beam weights vector, the asterisk denotes the conjugate of a complex vector or matrix, and μ is a constant. Furthermore, compute the sample covariance matrix via the simple "block" average taken over N snapshots,

$$\hat{\mathbf{R}} = \frac{1}{N} \sum_{n=1}^N [\mathbf{E}(n) \mathbf{E}(n)^*], \quad (2)$$

where $\mathbf{E}(n)$ is the element signal data vector received at the n th time sampling. (See Appendix I for description of snapshot signal model.) The data observation/integration time in (2) is the parameter N . If $\hat{\mathbf{R}}$ is estimated over a lengthy observation time, like thousands of snapshots, then the sidelobe fluctuations from \mathbf{W} updates will be relatively small. However, practical system usage often demands short observation times on the order of hundreds of snapshots or even less.

Fig. 1 illustrates typical adapted pattern behavior for independent estimates of $\hat{\mathbf{R}}$ using $N = 256$ snapshots per update for the case of three 30 dB noncoherent sources located at 14° , 18° , and 22° . The antenna aperture chosen for this example is a 16-element linear array with half-wavelength element spacing and a 30 dB Taylor illumination incorporated in \mathbf{S}^* . Note that the adaptive algorithm maintains the main beam region and successfully nulls out the interference sources, but that it also raises the sidelobe levels elsewhere. The adaptive patterns are in continual fluctuation in the sidelobe regions and may exceed the quiescent sidelobe level by a considerable margin. Also, the main beam suffers a significant modulation which would degrade tracking performance. These effects worsen as the value of N decreases.

To understand the reason for this undulating pattern behavior, it is helpful to analyze the optimum weights in terms of eigenvalue/eigenvector decomposition. A derivation of such a decomposition for (1) can be found in [1], and we reproduce here (B18).

$$\mathbf{W} = \mu' \left[\mathbf{S}^* - \sum_{i=1}^K \left(\frac{\beta_i^2 - \beta_0^2}{\beta_i^2} \right) \alpha_i \mathbf{e}_i \right] \quad (3)$$

where $\alpha_i = \mathbf{e}_i^* \mathbf{S}^*$ and $\mu' = \mu / \beta_0^2$.

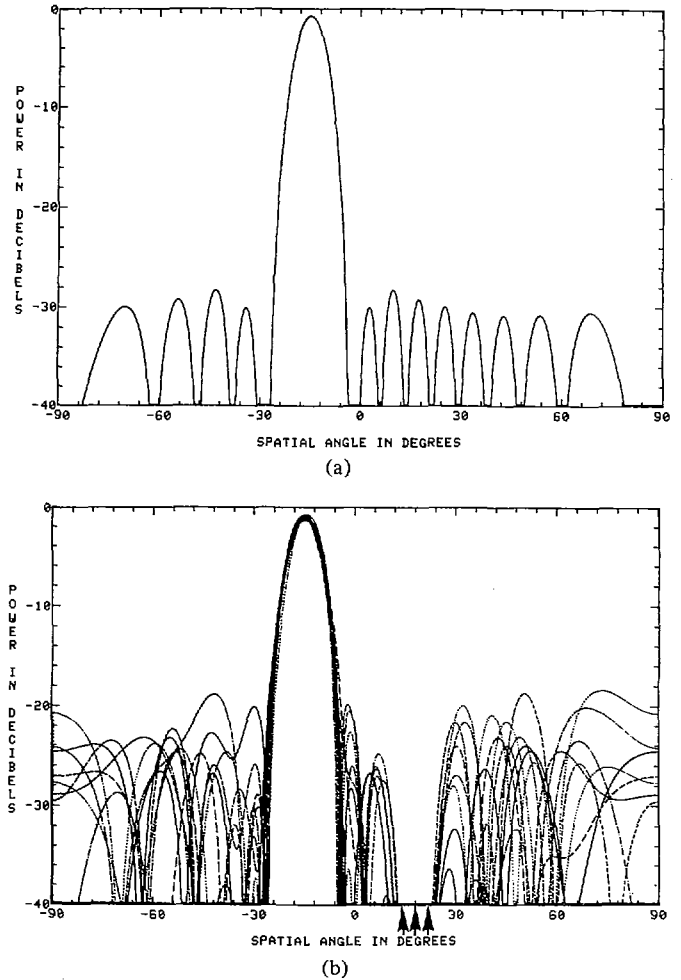


Fig. 1. Fully adaptive 16-element linear array, SMI algorithm with $\hat{\mathbf{R}}$ estimated from 256 snapshots per update, three 30 dB noncoherent sources located at 14° , 18° and 22° . (a) Quiescent main beam pattern, 30 dB Taylor weighting. (b) Typical adapted patterns, nine update trials plotted.

t denotes the transpose of a vector or matrix. The β_i^2 and \mathbf{e}_i are the eigenvalues and eigenvectors, respectively, of the sample covariance matrix, and β_0^2 is equal to receiver channel noise power level. Equation (3) shows that \mathbf{W} consists of two parts: the first part is the quiescent main beam weight \mathbf{S}^* ; the second part, which is subtracted from \mathbf{S}^* , is a summation of weighted, orthogonal eigenvectors. This is a clear expression of the fundamental principle of pattern subtraction which applies in adaptive array analysis. The reader is referred to [13] for a more extensive discussion.

We introduce the term principal eigenvectors (PE) to mean those eigenvectors which correspond to unique eigenvalues generated by the spatial source distribution; and the term "noise eigenvectors" to mean those eigenvectors which correspond to the small noise eigenvalues generated by the receiver channel noise contained in the finite $\hat{\mathbf{R}}$ estimates. The PE are generally rather robust and tend to remain relatively stable from one data trial to the next, whereas the noise eigenvectors tend to fluctuate considerably because of the inherent random behavior of noise. This difference in behavior is illustrated in Fig. 2 for the three source case described above, wherein there are three PE and 13 noise eigenvectors associated with each $\hat{\mathbf{R}}$ estimate. Fig. 2(a) shows the stability

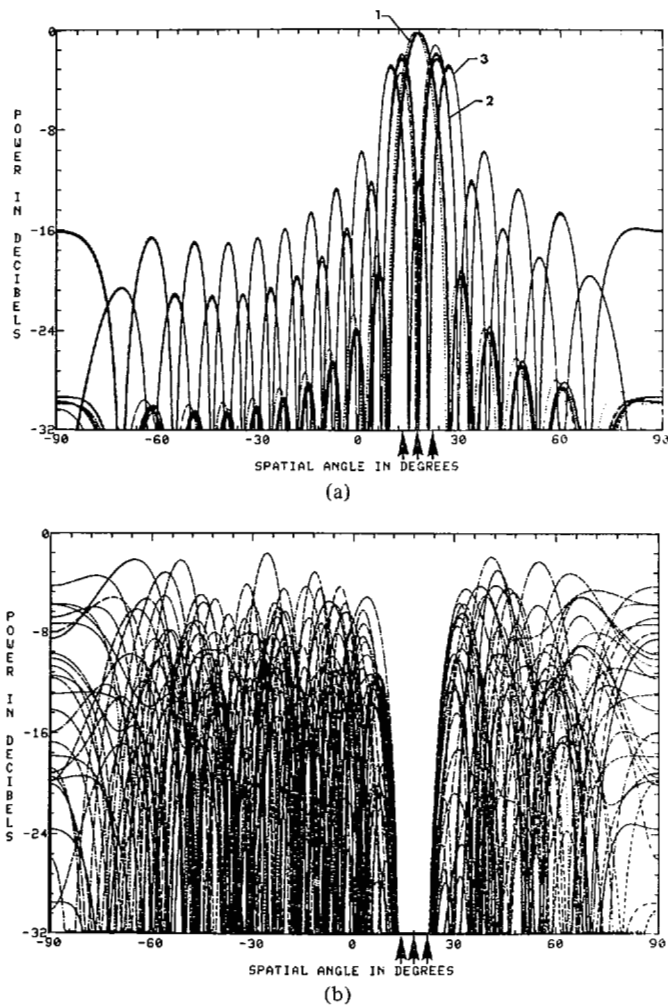


Fig. 2. Plots of principal eigenvectors and noise eigenvectors computed from the $\hat{\mathbf{R}}$ estimates associated with the three-source case of Fig. 1, nine update trials. (a) Principal eigenvectors 1, 2, and 3. (b) Typical noise eigenvectors 4, 10, and 16.

of the three PE for nine trials, and Fig. 2(b) shows the random behavior of typical noise eigenvectors for the exact same trials. Thus, we would expect that the sidelobe undulations in Fig. 1(b) are associated primarily with the noise eigenvectors. This thesis is verified in Fig. 3, which illustrates the adapted patterns resulting from (3) when only the PE are subtracted.

The above adaptive array pattern behavior leads to the following observations for source distributions which do not encroach upon the main beam and involve a small number of the available degrees of freedom.

1) It is possible to retain low sidelobes in the adapted patterns, even with short observation times, by constraining our algorithm (3) to utilize only the PE. The weight solution is unique and therefore stable.

2) Utilizing only the PE is tantamount to operating our adaptive system in beamspace (as opposed to element space) with a set of weighted orthogonal canceler beams.

3) The fully adaptive array automatically forms and "assigns" its PE canceler beams to cover the interference source distribution, with one beam per each DOF needed.

Therefore, we have set forth a low-sidelobe eigenvector constraint algorithm for this type of restricted interference situation.

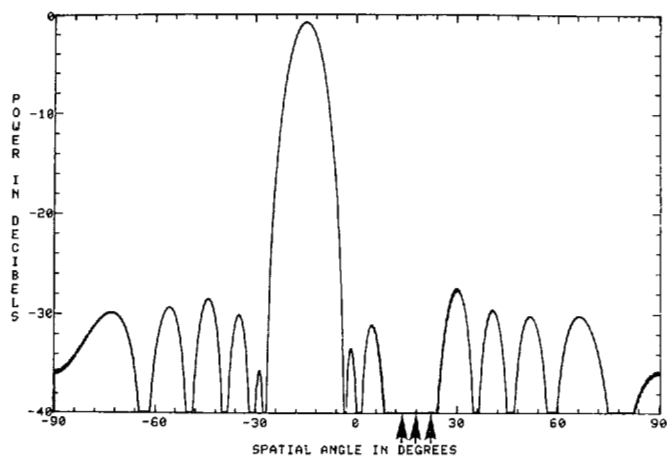


Fig. 3. Typical adapted patterns resulting from the constraint of utilizing only the PE, three-source case of Fig. 1.

B. Low-Sidelobe Constraints for a General Beamformer

Consider next a more interesting configuration shown by the schematic diagram of Fig. 4, where we represent an adaptive array system operating in beamspace so as to have available some preadaptation spatial filtering. Applebaum and Chapman [10], [14] first described beamspace systems of this type, utilizing a Butler matrix [15] beamformer wherein the vector of beamformer outputs $\hat{\mathbf{E}}$ may be expressed,

$$\hat{\mathbf{E}} = \mathbf{B}'\mathbf{E} \quad (4)$$

where \mathbf{B} is a $K \times K$ matrix containing the beamformer element weights. Other descriptions of beamspace systems are also available in the literature [11], [16], [17], [18], of which Adams *et al.* [17] is particularly germane to our discussion. Chapman [10] pointed out that when utilized in a partially adaptive configuration, such beamspace systems are susceptible to aperture element errors and cannot arbitrarily compensate the random error component of their sidelobe structure. This makes it necessary to control element errors in accordance with the quiescent main beam sidelobe level desired, and fits into our initial assumption of low-sidelobe design mentioned earlier. A separate weighted main beam summing is indicated which may be obtained either by coupling into the beamformer outputs as shown, or by coupling off from the elements and providing suitable phase shifters for steering plus a corporate feed network. Our purpose here is to examine the sidelobe performance of such a partially adaptive beamspace system in which element errors are kept low and beamformer beams are subjected to simple constraints.

Spatial estimation data on the interference source distribution shall determine which beamformer beams are to be adaptively controlled. Such beams are defined herein as "assigned" beams, and the idea is to assign only enough beams to accommodate the DOF required by the source distribution. Whenever the two are equal, the adaptive weight solution is unique and we avoid adding any extra "noisy" weight perturbations. The reader will recognize that we are attempting to replace the PE beams of Section II-A with assigned beams from our general beamformer. Thus, we are defining a partially adaptive array which will utilize only a relatively small number of its available DOF. In addition to

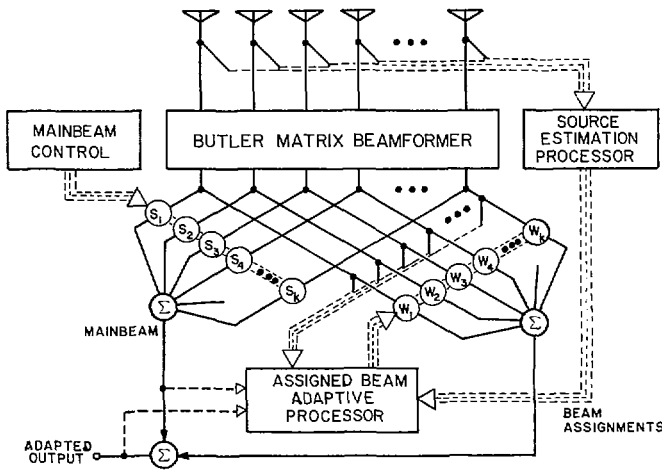


Fig. 4. Beamspace partially adaptive array with a separately weighted main beam and canceller beams assigned by a source estimation processor.

this assigned beam constraint, we seek to limit the adaptive weights of assigned beams to a maximum level γ chosen to exceed the mainbeam sidelobe level by only a few decibels. This prevents an excessive rise in adaptive sidelobe level, including the condition where the number of assigned beams exceeds the DOF required. γ actually represents the product of assigned beam gain and adaptive weight magnitude, such that we have the option of working with beamformer beams which are considerably decoupled/attenuated.

An equation formulation may be expressed in terms of the same pattern subtraction principle as utilized in (3) for K beams,

$$\mathbf{W}_0 = \mathbf{S}^* - \sum_{k=1}^K W_k \mathbf{b}_k \quad (5)$$

where $|W_k| \leq \gamma$ for J assigned beams and $W_k = 0$ for all other beams. \mathbf{b}_k is the k th Butler matrix beam element-weight vector. When $W_k = 0$, that beam port is essentially disconnected from the output summation and it is much to our advantage to reduce the DOF of the adaptive weight processor accordingly, i.e., this processor reduction relates directly to the computational burden, response time, sidelobe degradation, and overall cost mentioned earlier. For example, utilizing the SMI technique described in (1) and (2), we would now have the advantage that our sample covariance matrix of signal inputs $\hat{\mathbf{R}}$ involves only the J assigned beams and its dimensions reduce from $K \times K$ down to $J \times J$, thereby greatly easing the computation burden involved in obtaining its inverse [11]. The equivalent "steering vector" Λ per Applebaum [9] is also reduced to dimension J and consists of the cross correlation between the main beam signal V and the J assigned beam outputs \mathbf{Y}

$$\Lambda = \frac{1}{N} \sum_{n=1}^N V(n) \mathbf{Y}^*(n). \quad (6)$$

The j th assigned beam output for the n th snapshot signal sample is simply

$$Y_j(n) = \mathbf{E}^t(n) \mathbf{b}_k, \quad k \text{ set by } j \quad (7)$$

where the particular value of k must be selected for the j th assigned beam. Our J dimension adaptive weight solution thus becomes

$$\mathbf{W} = \hat{\mathbf{R}}^{-1} \Lambda. \quad (8)$$

Equation (8) gives us the J assigned beam weights required in (5). The proposed constraint $|W_k| \leq \gamma$ can be applied directly to the solution from (8), but recognize that this is a "hard" constraint and the results will not be optimal when the limit is exceeded.

A softer, more flexible constraint for our purposes is one suggested by Brennan¹ based upon Owsley [19], where one selects weights which simultaneously minimize both the output and the sum of the weight amplitudes squared, i.e.,

$$\text{minimize } \{ |\bar{V} - \bar{\mathbf{W}}^t \mathbf{Y}|^2 + \alpha \bar{\mathbf{W}}^t \mathbf{W}^* \}.$$

where the overbar denotes averaging over N snaps. The solution is a simple modification to (8) wherein

$$\mathbf{W} = [\hat{\mathbf{R}} + \alpha \mathbf{I}]^{-1} \Lambda \quad (9)$$

where $\alpha = (\gamma^2/J) \text{trace} [\hat{\mathbf{R}}]$.

Note that (9) adds a small percentage of the average assigned beam power to the diagonal terms of $\hat{\mathbf{R}}$, i.e., it is a "pseudonoise" addition technique. Recall that γ was selected to be close to the main beam sidelobe level. Although α is a small percentage of the trace $[\hat{\mathbf{R}}]$, it is generally much larger than the receiver noise level β_0^2 , and this domination over receiver noise by a constant will tend to severely dampen weight fluctuations due to noise. Of course, (9) deviates from the optimum Weiner weights and will result in a slightly larger output residue, but the cost is negligible compared to the remarkably stable results achieved from this rather simple constraint. It essentially permits the number of assigned beams to exceed the DOF required, and yet retain low sidelobe levels. Equations (5)–(9) were utilized in computing the adaptive pattern examples which follow. The reader should recognize that the J dimension adaptive weight solution may be arrived at via any of the current adaptive processing algorithms such as Howells–Applebaum [9], Gram–Schmidt [11], sample matrix inverse update [20], etc.

Applying these constraints to our three-source case of Fig. 1, we would assign beamformer beams 10, 11, and 12 to cover the sources, as illustrated in Fig. 5. These assigned beams are then given a maximum gain level about 5 dB above the -30 dB main beam sidelobes, or $|W_k| \leq 0.055$. All other W_k are set to zero. Typical resultant adapted patterns are almost identical to Fig. 3. The pattern stability is near-perfect for a unique solution like this, and note that the three sources have been nulled with very little perturbation of the mainbeam sidelobes except in the immediate vicinity of the sources. Since we are inverting a matrix of only 3×3 dimension in (8) for this case, it follows that the number of snapshots processed per trial could be reduced by an order of magnitude [12] and still have excellent results. The adaptive weights will tend to become "noisy" if we include even one extra DOF beyond the

¹ Private communication, L. E. Brennan, Adaptive Sensors, Inc.

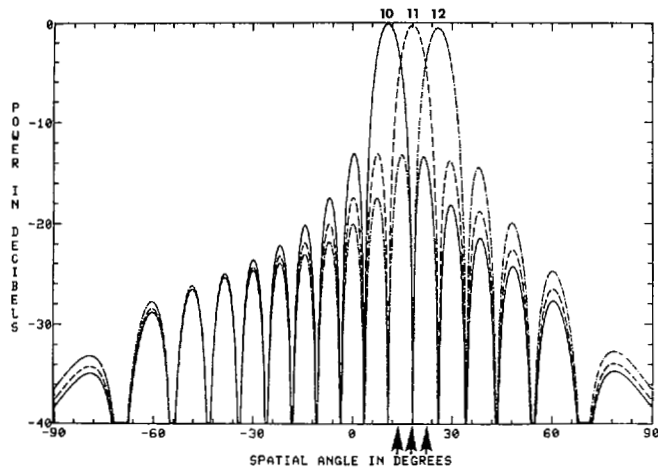


Fig. 5. Beamformer beams 10, 11, and 12 assigned to cover the three-source case of Fig. 1.

unique solution. However, if we use the "soft" constraint of (9) in solving for the weights, stable performance is again restored despite the extra DOF.

Although not shown here, another example of interest was the case of using a two-beam cluster (11 and 12 in Fig. 5) to cancel a single 40 dB broad-band source located at 22°. It was found that the source could be adequately cancelled at bandwidths up to 15 percent.

Many other combinations of source distributions and assigned beams were tested to further verify the technique, and the partially adaptive performance was satisfactory *provided that the assigned beams were sufficient to cover the DOF demanded by the source distribution.*

C. Interference Sources in the Main Beam Region

Extension of the foregoing partially adaptive array technique for main beam interference is straightforward, provided we relax the constraint upon the value of γ in (5). Obviously, the low-sidelobe strategem becomes secondary to the greater menace of an interference source coming in thru our high-gain main beam. Low sidelobes could still be retained, if necessary, by implementing a beamformer which is capable of producing a family of low-sidelobe assigned beams [17].

III. SOURCE ESTIMATION AND BEAM ASSIGNMENT

Modern spectral estimation techniques are considered complementary to the conventional methods for tracking and cataloging interference sources. They do not interfere with any functions of the main beam, and they are capable of providing superior source resolution from fewer elements. The latter advantage is gained in part because we assumed low sidelobes for the main beam, i.e., the only sources that require estimation are those few which are of sufficiently high SNR to get thru the mainbeam sidelobes. Resolution performance is always directly related to signal-to-noise ratio (SNR), of course [3], [7], [8].

The principle of achieving source estimation from a small fraction of the aperture DOF has been demonstrated via many techniques, both conventional and optimal [2], [4], [21]. It is not within the scope of this paper to attempt a comprehensive

comparison of such techniques, but the point is important to our concept so that an example of a half-aperture linear array estimator is given in this section. The type of application envisioned is illustrated in Fig. 6, where we represent a $K \times K$ element aperture system in which the adaptive beam DOF are to be assigned on the basis of estimates derived from two orthogonal linear arrays of $K/2$ elements each. An extension of the two-dimensional beamspace adaptive array system of Fig. 4 to the three-dimensional system suggested by Fig. 6 permits several beamformer options, including 1) two orthogonal two-dimensional beamformers of which one is coupled into a row and the other coupled into a column of elements; and 2) a complete three-dimensional beamformer [22] coupled into the aperture elements, perhaps on a thinned basis. The separate main beam must be summed from all K^2 elements in order to attain the desired low sidelobes.

Although they involve relatively few elements from the aperture, the linear array estimators represent a significant increase in system expense because they are all-digital processing subsystems. Processing of the digital signals to estimate the sources may be carried out in accordance with a number of spectral estimation algorithms available in the literature [1]–[8]. Several algorithms that were utilized in the simulations conducted for this paper are discussed in [1].

Once the source estimation information is available, then we can assign beamformer beams via a computer logic program. A Fortran IV computer code named "BEAMASSIGN" was developed which accepts source information updates, compares the new data against a source directory kept in memory, computes track updates for sources already in memory, determines priority ranking, and assigns beams to cover the sources of highest priority. An important point to note is that beam assignment does not require great accuracy, i.e., a half-beamwidth is usually close enough. Also, clusters of two or three adjacent beams may be assigned for doubtful cases.

A demonstration of beam assignment was conducted with a moving source simulation involving the 16-element linear array of Fig. 1. Four sources of unequal strength were set up in the far field, traveling in crisscrossing patterns. Two of the sources are of 30 dB strength with start angles of 3.0° and 39.0°, and two are of 43 dB strength with start angles of 5.0° and 70.0°. The estimation of the scanned main beam for this example is shown in Fig. 7(a). Each time-unit plot cut is computed from $\hat{\mathbf{R}}$ averaged over 160 snapshots,

$$P_0 = \mathbf{S}' \hat{\mathbf{R}} \mathbf{S}^* \quad (10)$$

where \mathbf{S}^* is the main beam steering vector used to generate the display plot. As expected, this simple Fourier output is dominated by the two stronger sources. In contrast, Fig. 7(b) shows the source estimation derived from eigenanalysis processing using only half of the aperture (eight elements). Note that the "superresolution" characteristics of this type of optimal estimation produces excellent source tracking, even in the vicinity of crossover of three of the sources.

The results of using the source information data contained in Fig. 7(b) to continuously update beam assignments is illustrated in the adapted pattern cuts shown in Fig. 8(a). Note that the main beam remains steady and the sidelobes seldom exceed

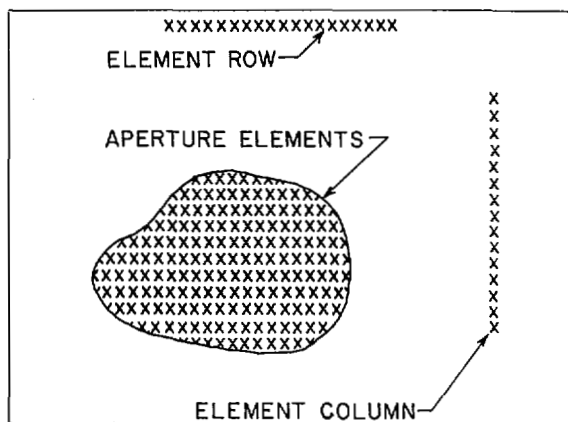


Fig. 6. $(K \times K)$ element aperture within which row/column linear arrays couple into source estimation processors.

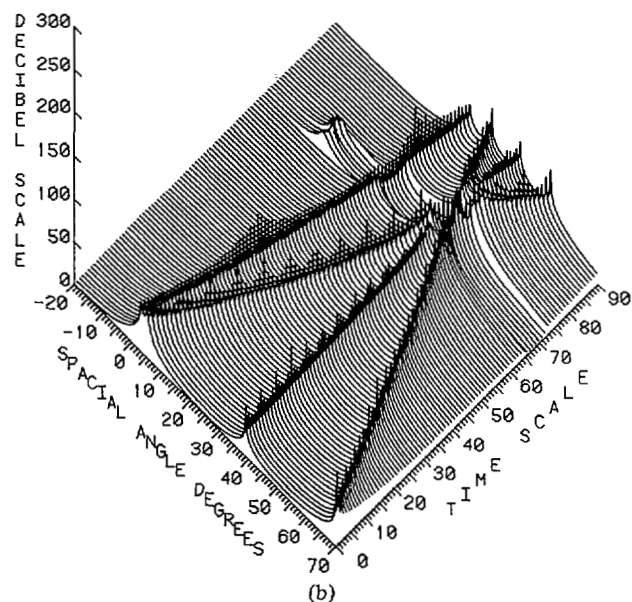
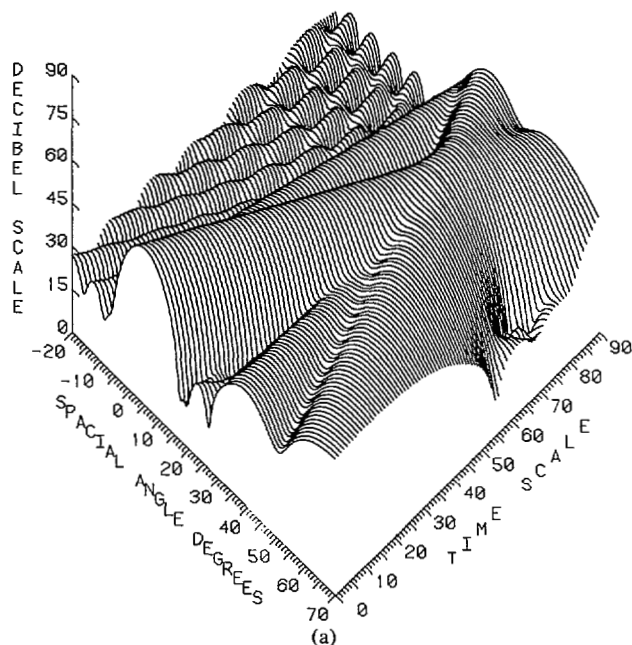


Fig. 7. Estimation of four moving sources via main beam scan and half-aperture eigenanalysis algorithm, 160 snapshots averaged per plot cut. (a) Conventional main beam scanning, 16 elements, 30 dB Taylor illumination. (b) Half-aperture eigenanalysis source estimation.

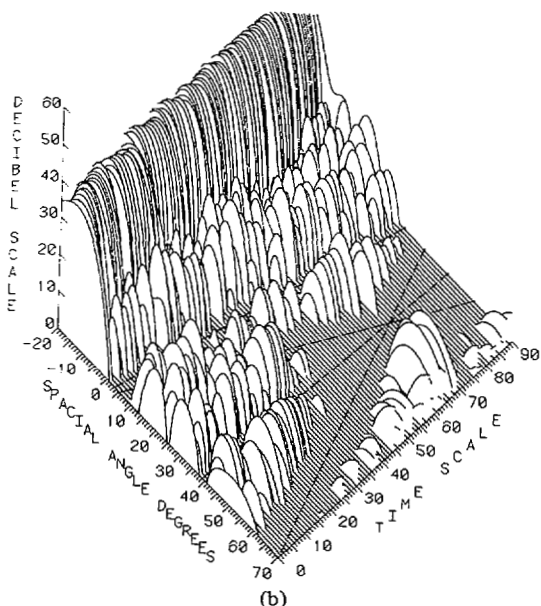
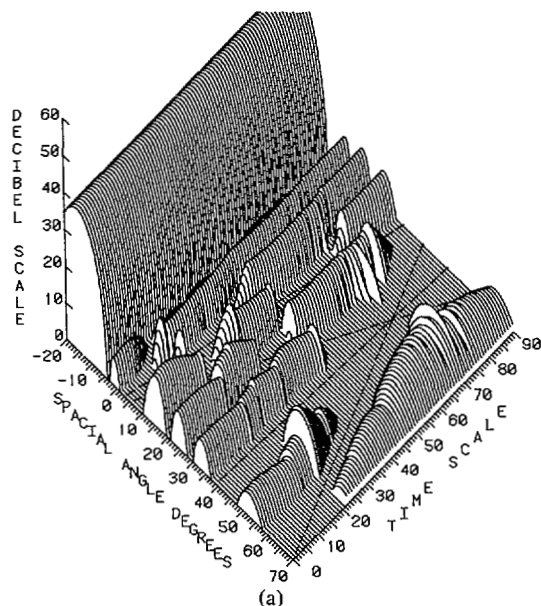


Fig. 8. Adaptive patterns for 16 element linear array, SMI algorithm, four moving sources case of Fig. 7. (a) Partially adaptive, constrained, assigned beams, 32 snapshots processed per plot cut. (b) Fully adaptive array, no constraints, 300 snapshots processed per plot cut.

their quiescent 30 dB peak level, despite the drastic shifting of the nulls as the moving sources crisscross in the sidelobe region. In contrast, Fig. 8(b) illustrates the adapted pattern cuts obtained when we utilize the SMI algorithm weights with the array fully adaptive. Although the source cancellation is excellent, the main beam suffers significant modulation and the peak sidelobe levels rise considerably.

IV. AN ADAPTIVE ARRAY TRACKING APPLICATION

A second area where spectral estimation techniques can provide valuable assistance is that of adaptive array tracking systems. Here we are dealing with the problem of attempting to track targets under the condition of having interference sources present in the main beam region. Some early proposed solutions in this area evolved from the growing adaptive array

technology of the 1970's. For example, a paper by White [23] discusses the radar problem of tracking targets in the low-angle regime where conventional tracking radars encounter much difficulty because of the presence of a strong surface-reflected ray.

The first extension of fully adaptive arrays to angle estimation in external noise fields is the contribution of Davis *et al.* [24], who developed an algorithm based on the outputs of adaptively distorted sum and difference beams. The adaptive beams filter (null) the external noise sources, and distortion correction is then applied in the resultant monopulse output angle estimate. Their work is particularly appropriate as a starting point for this section, where we discuss the advantages of using spectral estimation techniques in an all-digital, fully adaptive, array tracking system; [17] is also pertinent.

A. Coherent Spatial Interference Sources

The existence of significant coherence between spatial sources as, for example, in multipath situations involving a specular reflection, continues to represent a serious problem area even for a fully adaptive tracking array. Reasons include

- 1) coherent signals are not stationary in space [3], [7], [25];
- 2) adaptive systems may perform cancellation via weight phasing rather than null steering [7], [25]–[28];
- 3) adaptive tracking beam distortion is highly sensitive to coherent signal phasing;
- 4) signal fading under antiphase conditions.

To demonstrate these reasons, adaptive characteristics were computed for a 16-element linear array for an interference case in which there are two 13 dB coherent sources in the main beam region. There is also a third source, noncoherent, in the nearby sidelobe region to act as a stable null comparison point.

In Fig. 9, we illustrate the severe changes in our main beam caused by variation of the phase shift between the two coherent sources located at -7.6° and -4.0° . The quiescent main-beam has the same Taylor weighting as in Fig. 1(a). Note that for phasing of 0° and 180° , the adaptive weights are not achieving cancellation by steering nulls onto the coherent sources but, rather, by the weight phasing itself. The array output was driven down to receiver noise level for all three phases. The plots for 90° phase are very similar to what one would obtain if all three sources were noncoherent, i.e., cancellation is achieved by adaptive null steering in this instance.

Such severe sensitivity to coherent source phasing in the mainbeam region produces different distortions in tracking estimates from adaptive Σ (sum) and Δ (difference) patterns, as shown in Fig. 10. The equation development for this type of plot is in [1], but the main point here is to show the considerable changes in track angle estimates just due to phase variation. Once again, if all three sources were noncoherent, the distortion plot would be stable and very similar to the one shown for 90° phase.

B. All-Digital Tracking System Concept

The separate estimation of interference source data (total number, power levels, location angles, coherence) and its

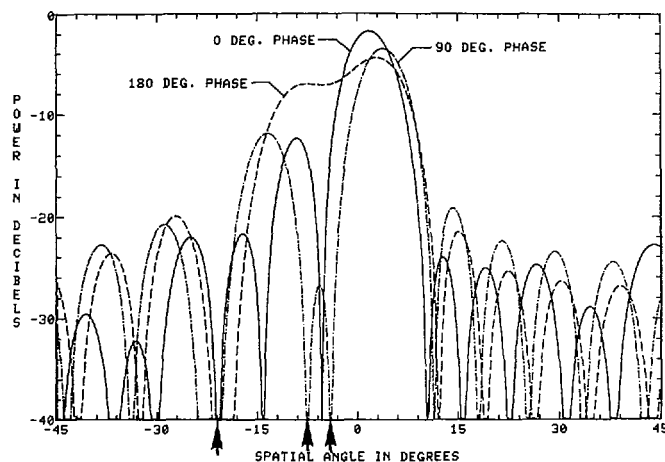


Fig. 9. Typical adaptive patterns for coherent interference in the mainbeam region; 16 element linear array, SMI algorithm, two 13 dB coherent sources located at -7.6° and -4.0° .

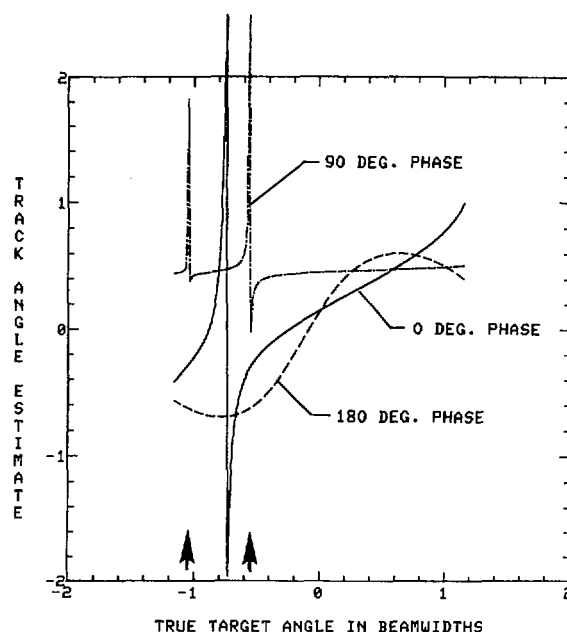


Fig. 10. Track estimate distortion resulting from adaptive Σ and Δ tracking beams for coherent interference in the main beam region, same case as Fig. 9.

utilization to improve the output SNR of desired signal detections is a mode of system operation that has been addressed in the literature a number of times for various applications [7], [8], [17], [18]. In this section, we briefly review such a system wherein the estimated data is used to drive a fully adaptive tracking processor [1]. The concept is illustrated in Fig. 11. Starting on the left side, the system continuously computes/updates a sample covariance matrix $\hat{\mathbf{R}}$. Of particular significance is the fact that $\hat{\mathbf{R}}$ may be dimensioned either equal to or less than the total number of array elements, i.e., the model order of the estimate is selectable per subaperture averaging option choice. Off-line processing on $\hat{\mathbf{R}}$ is then conducted at periodic intervals to estimate the locations and relative power levels of interference sources via the most appropriate spectral estimation algorithms. The central processor unit (CPU) then applies these data to the computation of optimized adaptive spatial filter weights for the right side of

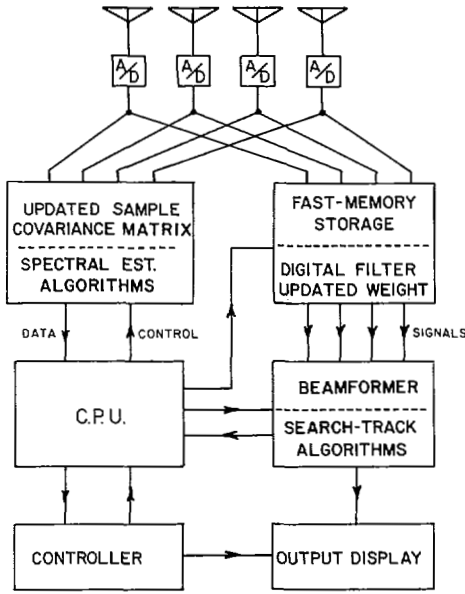


Fig. 11. All-digital adaptive array tracking system concept.

Fig. 11. Separation of source estimation from adaptive filter weight computation can be done accurately only in an all-digital processing system, but it permits the following benefits:

- 1) estimation of coherent interference source locations for deliberate adaptive null filter placement;
- 2) remembering slowly changing or time-gated sources;
- 3) anticipating sources from *a priori* data inputs;
- 4) flexibility in time-domain control of the filtering to counter interference time strategies;
- 5) tracking/cataloging/ranking sources;
- 6) efficient assignment of available DOF;
- 7) compatible with fast-response adaptive algorithms, i.e., parallel algorithm processing.

The right side of Fig. 11 indicates a fast-memory storage capability which is intended to permit selected time delays of the snapshots for feeding into the filter weights. The idea is to synchronize selected snapshots with their filter weight updates if possible.

Finally, the filtered signal output residue is fed into a beamformer which is weighted to produce the desired search and monopulse track beams for target detection and tracking. The algorithms of Davis *et al.* [24] may be applied for estimating the target signal angle of arrival, based upon the outputs of adaptively distorted sum and difference beams. Reference [1] discusses the equivalence of such beams to the Fig. 11 concept.

As an example, let us apply this concept to the coherent sources case utilized for Figs. 9 and 10 wherein we would utilize a 16-element linear array feeding into our all-digital processor. An appropriate estimation algorithm is that of forward-backward subaperture spatial smoothing [7], [28], [29], [30] combined with eigenanalysis. The rudiments of this algorithm are described in [1], and the results are plotted in Fig. 12 in comparison with a scanned main beam output. From

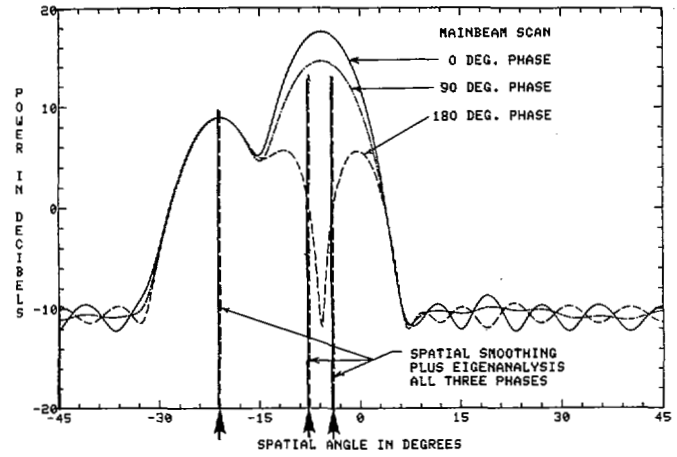


Fig. 12. Comparison of main beam scan versus spatial smoothing processing for coherent source case of Fig. 9, PEGS eigenanalysis, 256 snapshots per trial.

this source estimation data, we can construct an equivalent covariance matrix dimensioned for the full aperture per the procedure given in Appendix I, and compute its inverse for obtaining the adaptive filtering. If we define the constructed covariance matrix as \mathbf{M} , then its inverse may be viewed as a matrix set of adaptive "beamformer" filter weights to give us the filtered output n th snapshot vector $\mathbf{E}_f(n)$,

$$\mathbf{E}_f'(n) = \mathbf{E}'(n)\mathbf{M}^{-1}. \quad (11)$$

Conventional beam weighting \mathbf{S}^* can then be applied to the filtered output residue to obtain the final output for the n th snapshot,

$$Y_0(n) = \mathbf{E}_f'(n)\mathbf{S}^* = \mathbf{E}'(n)\mathbf{M}^{-1}\mathbf{S}^* \quad (12)$$

or

$$Y_0(n) = \mathbf{E}'(n)\mathbf{W}_0$$

where \mathbf{W}_0 is the familiar optimum Wiener filter weight.

Note that the constructed covariance matrix \mathbf{M} permits options such as adding synthetic sources or changing power levels. Furthermore, since it is always Toeplitz, solutions may be simplified somewhat.

For the current example, the computed adaptive characteristics would be very similar to those plotted in Figs. 9 and 10 for the 90° phase angle.

V. CONCLUSION

Two conceptual application areas have been presented for using spectral estimation techniques; partially adaptive low-sidelobe arrays, and fully adaptive tracking arrays. In both cases, improved spectral estimation techniques are used separately to acquire information about the interference environment which is beyond that ordinarily available in a conventional adaptive array. Examples discussed included "superresolution" effects, relative power level determination, estimation of coherent sources, and the tracking/cataloging/ranking of sources. For the partially adaptive area, the information was utilized for efficient assignment of a limited number of DOF in a beamspace constrained adaptive system in

order to obtain the following benefits (as compared to a fully adaptive array): retention of low sidelobes plus a stable mainbeam; considerably faster adaptive response; reduction in overall cost; and greater flexibility. On the negative side of the coin, we incur the risk of possible inferior cancellation performance if the interference source situation is not adequately covered by the assigned DOF.

For the fully adaptive tracking array area the information is utilized in an all-digital processing system to obtain the benefits of stable nulling of coherent interference sources in the main beam region, efficient assignment of the available DOF, and a far greater flexibility in the time-domain control of adaptive filtering strategy.

APPENDIX I

SNAPSHOT SIGNAL MODEL

Consider a simple linear array of K elements. The received signal samples are correlated in both space and time, giving rise to a two-dimensional data problem, but we convert this to spatial domain only by assuming that narrow-band filtering precedes our spatial domain processing. Bandwidth can be handled when necessary via a spectral line approach [13] or tapped delay lines at each element [20], but we did not consider such extra complication essential to the basic purposes of this analysis. Thus, the postulated signal environment on any given observation consists of I narrow-band plane waves arriving from distinct directions θ_i . The RF phase at the k th antenna element as a result of the i th source would be the product $\omega_i X_k$, where X_k is the location of the element phase center with respect to the midpoint of the array in wavelengths, and ω_i is defined as

$$\omega_i = 2\pi \sin \theta_i. \quad (13)$$

This notation is deliberately chosen to have the spatial domain dual of sampling in the time domain, so that the reader may readily relate to the more familiar spectral analysis variables. $\sin \theta_i$ is the dual of a sinusoid frequency f_i , and the X_k locations are the dual of time sampling instants t_k . Note that if our elements are equally spaced by a distance d , then X_k may be written,

$$X_k = \left(\frac{d}{\lambda} \right) \left(k - \left(\frac{K+1}{2} \right) \right) \quad (14)$$

where λ is the common RF wavelength. The ratio d/λ becomes the dual of the sampling time T with the cut-off frequency equal to the reciprocal.

The complex amplitude of the i th source at the array midpoint phase center is p_i , such that we can now express the n th time-sampled signal at the k th element as

$$E_k(n) = \eta_k(n) + \sum_{i=1}^I p_i(n) g_k(\theta_i) \exp(j\omega_i X_k) \quad (15)$$

where $g_k(\theta_i)$ is the element pattern response in the direction θ_i , and $\eta_k(n)$ is the n th sample from the k th element independent Gaussian receiver noise. (The receiver noise component is

assumed to be a random process with respect to both the time index n and the element index k .) Equation (15) permits us to construct a convenient column vector of observed data in the form,

$$\mathbf{E}(n) = \mathbf{V}\mathbf{p}(n) + \boldsymbol{\eta}(n) \quad (16)$$

where \mathbf{V} is a $K \times I$ matrix containing a column vector \mathbf{v}_i for each of the I source directions; i.e.,

$$v_{ik} = g_k(\theta_i) \exp(j\omega_i X_k). \quad (17)$$

Note that (16) separates out the basic variables of source direction in the direction matrix \mathbf{V} , source baseband signal in the column vector $\mathbf{p}(n)$, and element receiver channel noise in the column vector $\boldsymbol{\eta}(n)$. The vector $\mathbf{E}(n)$ is defined as the n th snapshot, i.e., a simultaneous signal sampling across all K -array elements at the n th time instant. These snapshots would nominally occur at the Nyquist sampling rate corresponding to our receiver bandwidth, so that a radar-oriented person may view them as range bin time samplings. However, for source estimation purposes, they need not necessarily be chosen from contiguous range bins and, in fact, for most applications it would be highly desirable to selectively time gate the snapshots used for source estimation. For this simple analysis, let us postulate that the snapshots are gated at more or less arbitrary instants of time.

Over typical processing intervals, the directions of arrival will not change significantly, so that \mathbf{V} is a slowly changing matrix. In contrast, the signals $p_i(n)$ will generally vary rapidly with time, often unpredictably, such that we must work with their statistical descriptions. It is assumed that the signals are uncorrelated with receiver noise. Proceeding then from (16), we can obtain the covariance matrix \mathbf{R} via application of the expected value operator \mathcal{E} , or ensemble average,

$$\mathbf{R} = \mathcal{E}[\mathbf{E}(n)\mathbf{E}^*(n)] \quad (18)$$

$$\mathbf{R} = \mathbf{V}\mathbf{P}\mathbf{V}^* + \mathbf{N} \quad (19)$$

where $\mathbf{N} = \mathcal{E}[\boldsymbol{\eta}(n)\boldsymbol{\eta}^*(n)]$, $\mathbf{P} = \mathcal{E}[\mathbf{p}(n)\mathbf{p}^*(n)]$, the asterisk is the complex conjugate, and t is the transpose. \mathbf{N} is a simple diagonal matrix consisting of the receiver channel noise power levels. The diagonal elements of \mathbf{P} represent the ensemble average power levels of the various signal sources, and off-diagonal elements can be nonzero if any correlation exists between the sources. Note that correlated far-field signals can easily arise if significant specular reflection or diffraction multipath is present.

REFERENCES

- [1] W. F. Gabriel, "Using spectral estimation techniques in adaptive processing antenna systems," Naval Res. Lab. Rep. 8920, Oct. 1985.
- [2] D. G. Childers, Ed., *Modern Spectrum Analysis*. New York: IEEE Press, 1978.
- [3] W. F. Gabriel, "Spectral analysis and adaptive array superresolution techniques," *Proc. IEEE*, vol. 68, pp. 654-666, June 1980.
- [4] Special Issue on Spectral Estimation, *Proc. IEEE*, vol. 70, Sept. 1982.
- [5] S. Y. Kung, H. J. Whitehouse, and T. Kailath, Eds., *VLSI and Modern Signal Processing*. Englewood Cliffs, NJ: Prentice-Hall, 1985.
- [6] R. Schmidt, "Multiple emitter location and signal parameter estima-

- tion," in *Proc. RADC Spectrum Estimation Workshop*, RADC-TR-79-63, Rome Air Development Center, Rome, NY, Oct. 1979, p. 243.
- [7] J. E. Evans, J. R. Johnson, and D. F. Sun, "Application of advanced signal processing techniques to angle of arrival estimation in ATC navigation and surveillance systems," MIT Lincoln Lab. Tech. Rep. 582, (FAA-RD-82-42), June 1982.
 - [8] A. J. Barabell *et al.*, "Performance comparison of superresolution array processing algorithms," MIT Lincoln Lab. Rep. TST-72, May 1984.
 - [9] S. P. Applebaum, "Adaptive arrays," *IEEE Trans. Antennas Propagat.*, vol. AP-24, pp. 585-598, Sept. 1976.
 - [10] D. J. Chapman, "Partial adaptivity for the large array," *IEEE Trans. Antennas Propagat.*, AP-24, pp. 685-696, Sept. 1976.
 - [11] R. A. Monzingo and T. W. Miller, *Introduction to Adaptive Arrays*. New York: Wiley, 1980.
 - [12] I. S. Reed, J. D. Mallett, and L. E. Brennan, "Rapid convergence rate in adaptive arrays," *IEEE Trans. Aerosp. Electron. Syst.*, vol. AES-10, pp. 853-863, Nov. 1974.
 - [13] W. F. Gabriel, "Adaptive arrays—An introduction," *Proc. IEEE*, vol. 64, pp. 239-272, Feb. 1976.
 - [14] S. P. Applebaum and D. J. Chapman, "Adaptive arrays with mainbeam constraints," *IEEE Trans. Antennas Propagat.*, vol. AP-24, pp. 650-662, Sept. 1976.
 - [15] J. Butler, "Multiple beam antennas," Sanders Assoc. Internal Memo RF 3849, Jan. 1960.
 - [16] J. T. Mayhan, "Adaptive nulling with multiple-Beam antennas," *IEEE Trans. Antennas Propagat.*, vol. AP-26, pp. 267-273, Mar. 1978.
 - [17] R. N. Adams, L. L. Horowitz, and K. D. Senne, "Adaptive main-beam nulling for narrow-beam antenna arrays," *IEEE Trans. Aerosp. Electron. Syst.*, vol. AES-16, pp. 509-516, Jul. 1980.
 - [18] E. C. DuFort, "An adaptive low-angle tracking system," *IEEE Trans. Antennas Propagat.*, vol. AP-29, pp. 766-772, Sept. 1981.
 - [19] N. L. Owsley, "Constrained adaption," in *Array Processing Applications to Radar*. New York: Academic, 1980.
 - [20] E. Brennan, J. D. Mallett, and I. S. Reed, "Adaptive arrays in airborne MTI radar," *IEEE Trans. Antennas Propagat.*, vol. AP-24, pp. 607-615, Sept. 1976.
 - [21] B. M. Leiner, "An analysis and comparison of energy direction finding systems," *IEEE Trans. Aerosp. Electron. Syst.*, vol. AES-15, pp. 861-873, Nov. 1979.
 - [22] J. P. Shelton, "Focusing characteristics of symmetrically configured bootlace lenses," *IEEE Trans. Antennas Propagat.*, vol. AP-26, pp. 513-518, July 1978.
 - [23] W. D. White, "Low-angle radar tracking in the presence of multipath," *IEEE Trans. Aerosp. Electron. Syst.*, vol. AES-10, pp. 835-853, Nov. 1974.
 - [24] R. C. Davis, L. E. Brennan, and L. S. Reed, "Angle estimation with adaptive arrays in external noise fields," *IEEE Trans. Aerosp. Electron. Syst.*, vol. AES-12, pp. 179-186, Mar. 1976.
 - [25] W. D. White, "Angular spectra in radar applications," *IEEE Trans. Aerosp. Electron. Syst.*, vol. AES-15, pp. 895-899, Nov. 1979.
 - [26] A. Cantoni and L. Godara, "Resolving the directions of sources in a correlated field incident on an array," *J. Acoust. Soc. Am.*, vol. 64, pp. 1247-1255, 1980.
 - [27] B. Widrow *et al.*, "Signal cancellation phenomena in adaptive antennas: Causes and cures," *IEEE Trans. Antennas Propagat.*, vol. AP-30, pp. 469-478, May 1982.
 - [28] T. J. Shan and T. Kailath, "Adaptive beamforming for coherent signals and interference," *IEEE Trans. Acoust., Speech, Signal Processing*, vol. ASSP-33, pp. 527-536, Jun. 1985.
 - [29] A. H. Nuttall, "Spectral analysis of a univariate process with bad data points, via maximum entropy and linear predictive techniques," Naval Underwater Syst. Center, New London, CT, NUSC-TR-5303, Mar. 1976.
 - [30] L. Marple, "A new autoregressive spectrum analysis algorithm," *IEEE Trans. Acoust., Speech, Signal Processing*, vol. ASSP-28, pp. 441-454, Aug. 1980.

William F. Gabriel (S'45-A'46-M'55-SM'59-F'82), for a photograph and biography please see page 275 of this issue.